Investigation of Loosely Bound States of NO_2 Just below the First Dissociation Threshold†

Antoine Delon*

Grenoble High Magnetic Field Laboratory, CNRS, BP 166 X, 38042 Grenoble Cedex 9, France

Florian Reiche and Bernd Abel

Institut für Physikalische Chemie, Universität Göttingen, Tammannstr. 6, 37077 Göttingen, Germany

Sergy Yu. Grebenshchikov and Reinhard Schinke

M.P.I. für Strömungsforschung, Bunsenstrasse 6, D-37073 Göttingen, Germany

Received: March 30, 2000

Loosely bound states of jet cooled NO_2 just below the first dissociation threshold D_0, with binding energies E_b between 0.8 and 59.3 cm^{-1}, have been investigated using pulsed VIS/UV optical double resonance spectroscopy. The measured UV spectra of these states in a spectral region where free NO absorbs have been found to depend strongly on the binding energy $E_b = D_0 - E$. This suggests that the states just below the dissociation threshold D_0 may be regarded (at least in part) to belong to a family of states corresponding to a large amplitude motion of an "oxygen atom" and a "NO fragment". Such states, typical for loosely bound nonrigid molecules or van der Waals complexes, are unusual for chemically bound molecules. In this paper we are describing first experiments in which we obtained direct evidence for their existence in NO_2. Most of the absorptions from the loosely bound states terminate on a dissociative potential energy surface (PES), so that the corresponding spectrum is a broad unstructured feature, with a blue shift (compared to free NO) increasing with binding energy. Very weak bound−bound transitions have also been observed. The analogy to spectra of NO/Ar van der Waals complexes is discussed.

I. Introduction

Features and the dynamics of highly excited vibrational states in polyatomic molecules play a major role for our understanding of reactive processes in molecular physics.[1,2] NO_2 is one of the model systems in molecular dynamics which became a prototype test system for many experimental as well as theoretical approaches. However, studying highly excited vibrational states of nitrogen dioxide, NO_2, remained a challenge for experimentalists and theoreticians. At low excitation energies, the molecules motion is well approximated by normal mode vibrations around the equilibrium configuration. This means that the vibronic eigenstates are uniquely assignable in terms of a complete set of quantum numbers (one electronic and three vibrational). As the excitation energy increases, especially above the conical intersection between the two lowest electronic states (around 10 000 cm^{-1}), the motion becomes more complex and the vibronic eigenstates start to lose their assignability.[3−5] Many groups have contributed to the elucidation of the spectroscopy of this molecule. Therefore, a complete overview is beyond the scope of this paper. As the excitation energy approaches the first dissociation threshold ($D_0 = 25\,128.57$ cm^{-1}),[6] the rovibronic eigenstates become completely unassignable and the usual spectroscopic selection rules are destroyed.[7] Recently, it was also found that in a narrow energy range spanning the last 20 cm^{-1} below D_0 the density of bound states grows suddenly by a factor of about five.[7] This discovery was the motivation for suggesting that very close to (but below) D_0 there may exist (in addition to "normal" mixed (chaotic) states) a family of states corresponding to another new type of motion: the large amplitude motion of almost free rotation of an O atom around the NO occurring at large average "interfragment" distances (|O...NO| > 7 Å).[8] The features of these states are particularly interesting because they sensitively probe the long-range part of the PES[9] (e.g., the multipole interactions on the ground state PES and features of the many almost degenerate excited state PESs at long internuclear distances), a region where the potential is usually not easily accessible by spectroscopic techniques because of unfavorable Franck−Condon factors (FCFs). Therefore, such states, typical for loosely bound nonrigid molecules or van der Waals complexes,[10] have not been observed in chemically bound molecules such as NO_2. In this paper we are describing an experimental strategy to probe these states in highly excited NO_2. We will show in this paper that most of the very loosely bound states of the NO_2 molecule (the binding energy being typically 1000th of the whole potential well depth) can be understood qualitatively in a simple local mode picture in which the states are assumed to correlate with a large amplitude motion along the interfragment distance or an orbiting motion of two "fragments", NO and O, around each other. In an "ideal" experiment one would like to probe the NO local mode character in highly excited NO_2 close to D_0 in a suitable VIS/IR (or VIS/MW) double resonance experiment, as was done to investigate the OH local mode character in highly excited HNO_3[11] and H_2O_2.[12] Instead, we used electronic double resonance spectroscopy[3] within the highly excited states of NO_2. Just as in electronic spectroscopy of weakly bound complexes we were looking for electronic transitions from the loosely

† Part of the special issue "C. Bradley Moore Festschrift".

* Corresponding author. E-mail: adelon@labs.polycnrs-gre.fr. Membre junior de l'Institut universitaire de France.

10.1021/jp001217i CCC: $19.00
Published on Web 08/25/2000

bound states to some unknown excited states in the vicinity of the strong $\gamma(0,0)$ transition of free NO.[13] With this strategy we probed the electronic "chromophore" of NO in highly excited NO_2. The main result of the experiments reported here is that several broad and narrow spectral features in the spectral range near 225 nm could be observed and attributed to transitions from the weakly bound eigenstates (low J) of NO_2 close to D_0 to unknown bound or short-lived excited states (in the following, abbreviated as bound−bound or bound−free transitions). We want to emphasize here that the approach we describe here resembles to some extent the UV− spectroscopy of a van der Waals complex.

The paper is organized as follows. First, we describe the experimental approach and the experimental technique as well as the proposed features of loosely bound states in chemically bound molecules. Then, we discuss spectra of 43 loosely bound states close to D_0 corresponding to different binding energies $E_b = D_0 - E$, ranging from 0.8 to 59.3 cm^{-1}. Finally, a simple theoretical approach as well as its limitations are described to rationalize the observed spectra and the similarities to weakly bound states of van der Waals complexes are discussed.

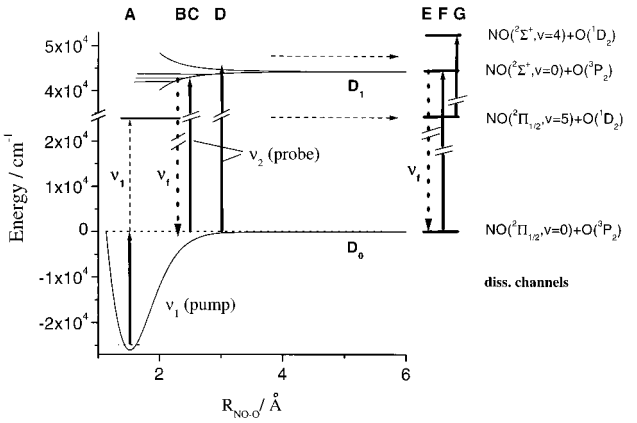

Figure 1. 1-D scheme of the experimental principle and of the involved PESs. A first ν_1 photon (A) pumps the NO_2 molecule from the ground state to some very loosely bound state below D_0. The ν_2 probe photon (C and D) promotes the molecule to some energy shell around the dissociation threshold D_1. The UV-LIF (B and E) is recorded as a function of ν_2 for different ν_1 frequencies. Energies are given approximately relative to D_0. The zero point energy of the NO spectator bond is not taken into account in the energy diagram.

II. Experimental Approach

A. Concept of Loosely Bound States in Chemically Bound Molecules and Their Probe. In the case of diatomic molecules and molecular complexes the properties of loosely bound states have been extensively studied in the past and are relatively well-known.[10,14,15] Although, such states can also be expected in chemically bound polyatomic molecules near dissociation thresholds[16] they are in general difficult to investigate experimentally because of the difficulties to detect them. Since FCFs are typically unfavorable for direct optical excitation of loosely bound states, either multiple resonance techniques have to be used or the molecule must exhibit sufficient intramolecular couplings to mix these states with optically bright states. NO_2 clearly corresponds to the latter case, since strong couplings between the levels of the first electronic excited state and high lying levels of the electronic ground state cause rovibronic chaos close to the first dissociation threshold.[4,5,7] This situation and the fact that the maximum absorption of the $\tilde{A}^2B_2 \leftarrow \tilde{X}^2A_1$ system is located close to D_0 enables us to excite almost all eigenstates of NO_2 at sufficient high internal energies and in particular close to D_0.[17] The strategy for the detection of a large amplitude motion signature is to search transitions originating from the loosely bound states of NO_2 in the UV which are close to transitions of the corresponding free fragments, NO ($^2\Pi_{1/2}$, $v = 0$, $J = {}^1/_2$) and O ($^3P_2$). Among the various possible spectroscopic features, a convenient one is the strong electronic $A^2\Sigma^+ \leftarrow X^2\Pi_{1/2}$ absorption spectrum of NO. The simple (very likely oversimplified) picture we adopt here to visualize our strategy is that we are looking for spectroscopic signatures and features of a "NO prefragment" perturbed by the surrounding oxygen atom. In section III we will discuss also the limitations of this picture.

To describe large amplitude motion states in NO_2, we employ a very simple local mode picture from cluster physics based on Jacobi coordinates. In this case R is the distance between the diatom center of mass and the dissociating atom, r is the diatom bond length and γ is the angle between the vectors associated with R and r. When the molecule is excited in a state very close to the dissociation threshold the energy is distributed over the 3 vibrational degrees of freedom. However, two distinct situations may be discussed. First, the available internal energy E (corresponding to a "binding energy" $E_b = D_0 - E$) of the molecule is shared democratically between the 3 vibrational degrees of freedom. Therefore, in a zeroth order picture the modes, on average, are excited by many quanta and the molecule will not explore large r and R distances. In addition, one may imagine a different situation in which 2 vibrational degrees of freedom (γ, R) can experience unusual wide amplitude motions of low frequencies, if the vibrational degree of freedom r is not excited and decoupled.[18] In this case the remaining bond (correlated with r) can be considered as a spectator bond corresponding to a high frequency motion (possibly similar to a fundamental) but containing on average no energy except zero point energy. In such a case the molecule may indeed explore large values of R or γ (the bending−hindered rotor coordinate). Since γ can explore the whole range between 0 and π, also weakly bound "orbiting states"[16] can be described in such a picture. Of course, one could also imagine a third situation in which all the internal energy is localized in only one degree of freedom. The key point here is that, due to the long-range part of the PES, the contribution of the states having large amplitude motion along R or γ and no excitation in the spectator bond, dominates (in terms of level density) the bound state spectrum in the vicinity of the dissociation threshold.[8] The wave functions corresponding to the weakly bound states therefore are very likely delocalized with maxima at large R. In addition, these states are most sensitive to the long range potential of the ground state and the several asymptotic electronically excited states at large R. *The hypothesis we are using in this study is that, the closer the UV electronic spectra from the investigated states are to the electronic spectra of free NO, the more delocalized are the states and the more is the loosely bound parent molecule almost resembling an NO:::::O complex. We further assume that the more delocalized the wave functions and the further out their maxima are, the larger is the FCF of the UV transitions in the asymptotic limit of the fragments at large R.* This situation is also depicted in Figure 1 where details of our pump and probe technique are displayed. To clarify terms we call D_1 the dissociation threshold energy of $NO_2 \rightarrow NO$ ($^2\Sigma^+$, $v = 0$, $J = {}^1/_2$) + O ($^3P_2$), $D_1 = D_0 + 44\,199.01\ cm^{-1} = 63\,927.58\ cm^{-1}$, where 44 199.01 cm^{-1} is the $Q_{1/2}$ transition of the $\gamma(0,0)$ band of NO.[13] In addition, two dissociation thresholds lie between D_0 and D_1: (i) $NO_2 \rightarrow NO$ ($^2\Pi_{1/2}$, $v = 0$, $J = {}^1/_2$) + O ($^1D_2$) at 40 996.5 cm^{-1} and (ii) $NO_2 \rightarrow NO$ ($^2\Pi_{1/2}$, $v = 0$, $J = {}^1/_2$) + O

($^1S_0$) at 58 921.2 cm^{-1}. They correspond respectively to the excitation energies of O ($^1D_2$), 15 867.9 cm^{-1} and of O ($^1S_0$), 33 792.6 cm^{-1} .[19] We will see in section III and in the Appendix that the lowest of these two thresholds plays a role for the "unwanted" 2-photon spectra.

As displayed in our pump and probe scheme in Figure 1 a first photon at frequency ν_1 promotes the rotationally cold NO_2 molecules ($J \sim {}^1/_2$) to loosely bound levels lying slightly below the first dissociation threshold D_0 of the electronic ground state $\tilde{X}^2A_1$ with low angular momenta $J = {}^1/_2$ and ${}^3/_2$ (A in Figure 1). This simple direct excitation process is possible because (i) the first excited electronic state of NO_2, $\tilde{A}^2B_2$, absorbs strongly in the visible range[17] and (ii) due to strong vibronic and rovibronic intramolecular couplings between the levels of $\tilde{X}^2A_1$ and $\tilde{A}^2B_2$,[4,5] its oscillator strength is distributed among the highly excited levels of $\tilde{X}^2A_1$, making them as observable as those of $\tilde{A}^2B_2$. The binding energy $E_b = D_0 - h\nu_1$ has been varied from 0.8 to 59.3 cm^{-1}. A second photon (C and D in Figure 1), at a frequency ν_2 close to the $A^2\Sigma^+$ ($v = {}^1/_2$, $J = {}^1/_2$) ← $X^2\Pi_{1/2}$ ($v = 0$, $J = {}^1/_2$) NO transition, can excite the loosely bound NO_2 molecules to (i) bound vibrational levels of a binding PES (if $h\nu_1 + h\nu_2 < D_1$), (ii) resonances of a binding PES (if $h\nu_1 + h\nu_2 > D_1$), and (iii) scattering states of a repulsive PES (if $h\nu_1 + h\nu_2 > D_1$).[20] We want to point out that the detected fluorescence signal in the latter two cases originates from electronically excited NO* (E in Figure 1) but in the first case originates from highly excited NO_2* (B in Figure 1). For the discussion and examination of spectra several other processes are important which are also displayed in Figure 1. First, since some cold free NO is always seeded in the sample it can be detected via 1-photon excitation at 226 nm (F in Figure 1). The corresponding spectrum consists of three sharp lines which can be discriminated easily. Second, due to 2-photon excitation, small quantities of NO are produced, both in the ground and vibrationally excited state ($v = 5$). The latter absorbs unfortunately in the wavelength region near 225 nm as well (G in Figure 1). We will discuss these interfering lines in section III and in the Appendix.

B. Experimental Setup. The experimental apparatus used in the present study is similar to those used in previous reports from our laboratory,[3,21,22] so we only briefly describe the salient features of the experiment. A mixture of 0.05% NO_2 in Helium at a backing pressure of 5−6 bar is expanded into the sample cell (residual pressure 10^{-4} mbar) through a pulsed nozzle (General Valve), thereby cooling the rotational degrees of freedom of NO_2 down to ca. 2 K. The NO_2 molecules are then excited to energy levels just below the dissociation threshold D_0 with laser pulses around 25100 cm^{-1} (2 mJ, 7 ns, fwhm 0.3 cm^{-1}) generated by a YAG/dye laser combination (Spectra Physics GCR 150/Lambda Physik Scanmate 2E, Exalite 398). The wavelength of the excitation pulses is calibrated and checked by a pulsed wavemeter (Burleigh WA 5500). To obtain a 1-photon overview spectrum of the threshold region (also for normalization purposes) laser-induced fluorescence (LIF) spectrum has been recorded as a function of the pump frequency ν_1, between D_0 and $D_0 - 60$ cm^{-1}, to find the various excitation lines on which the pump laser can be parked when scanning the frequency ν_2.

For the probe of the loosely bound states of NO_2 close to D_0 a second laser pulse at 44300 cm^{-1} (1 mJ, 10 ns), shifted by 50 ns in time, has been employed by using the frequency doubled output of a XeCl-excimer/dye laser combination (Lambda Physik Compex/Lambda Physik FL 3000, Coumarin 47). This frequency was calibrated against the well-known transitions of the free NO in the jet and against our Burleigh wavemeter. The energy of each of these pulses was recorded using an integrating photodiode. Both laser pulses are overlapped in the sample cell through baffled sidearms equipped with quartz windows at Brewster angle. The UV-LIF of the excited molecules is recorded at 90° to the incident laser beams by a *f*/1.2 condensor lens with a 50 mm focal length, filtered by a UG 11 UV transmitting filter and imaged onto the slit of a UV sensitive photomultiplier (EMI 9635QB). The PMT signal is then integrated and transferred to a PC for further processing. Usually about 10 pulses are averaged to form a single data point in the spectrum. NO_2 and Helium are purchased from Messer-Griesheim and used without further purification.

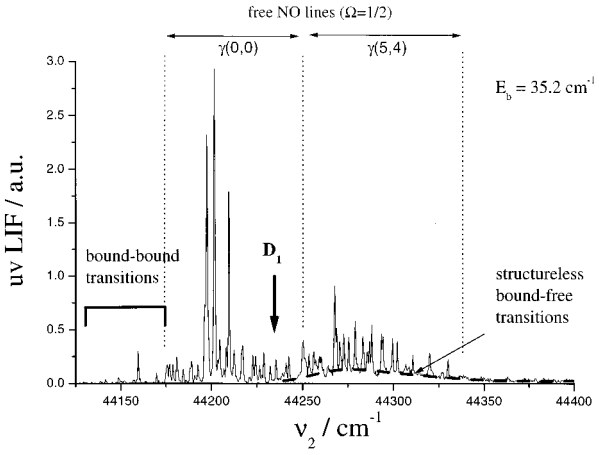

Figure 2. Example of a typical spectrum for a binding energy E_b = 35.2 cm^{-1}. The main features are: (i) three intense lines at about 44 200 cm^{-1} from cold NO (γ(0,0) lines); (ii) γ(0,0) lines of NO produced by 2-photon absorption and photodissociation, between 44 175 and 44 250 cm^{-1}; (iii) γ(5,4) transitions of NO for $\nu_2 >$ 44 250 cm^{-1} from the sequential 2-photon photodissociation of NO_2 (the NO ($^2\Pi_{1/2}$, $v = 5$) + O ($^1D_2$) threshold is located at 50 096.3 cm^{-1}); (iv) the broad absorption located between 44 200 and 44 400 cm^{-1}; (v) bound−bound transitions originating from the loosely bound states of the ground electronic state to the bound region of the unknown excited PES, for $\nu_2 <$ 44 175 cm^{-1}.

A total of 43 UV-LIF spectra have been recorded by tuning the probe frequency ν_2 for a fixed value of the pump frequency ν_1. These spectra have been normalized versus the pulse energy of the probe laser, which may change significantly during a scan (contrary to the energy of the pump laser which is very stable).

III. Results and Discussion

A. Decomposition of Experimental Spectra. In this section we first describe the various features which appear in our 43 experimental spectra in order to extract the information connected with the loosely bound states. The corresponding binding energy, $E_b = D_0 - h\nu_1$, of the states excited ranged from 0.8 to 59.3 cm^{-1}. The chosen ν_1 frequencies are those of the main NO_2 transitions appearing in this energy range of the visible LIF spectrum. Each of the spectra is recorded, for a fixed value of the frequency ν_1 of the pump beam, by scanning the frequency ν_2 of the probe beam from about 44 130 cm^{-1} to 44 420 cm^{-1}. This range includes the $A^2\Sigma^+$ ($v = 0$) ← $X^2\Pi_{1/2}$ ($v = 0$) vibrational band of NO (γ(0,0) $\Omega = {}^1/_2$ band), and also (accidentally) the γ(5,4) band of vibrationally excited NO. We show in Figure 2 a typical spectrum obtained for states close to D_0 with E_b = 35.2 cm^{-1}. The main information is somewhat obscured by lines of free NO due, either to 2-photon photodissociation of NO_2 (producing rotationally excited γ(0,0) and

$\gamma(5,4)$ bands) or to cold NO in the sample (producing rotationally cold $\gamma(0,0)$ band). The characteristic spectral features of the loosely bound states are the broad structureless absorption appearing as a "background" of the $\gamma(5,4)$ lines and the narrow lines on the low energy side of the $\gamma(0,0)$ $\Omega = {}^1/_2$ band head. Unfortunately, it was not possible yet to completely avoid the "unwanted" transitions, $\gamma(0,0)$ and $\gamma(5,4)$, in the experiment. However, the spectral features correlating with the loosely bound states of NO_2 depend on both laser frequencies ($\nu_1 + \nu_2$) and therefore shift in the ν_2 spectrum if ν_1 (and thus $E_b = D_0 - h\nu_1$) is varied. Conversely, all lines belonging to free NO (either cold or rovibrationally excited) are stationary and do not move in the ν_2 spectrum upon changes in ν_1. A more detailed discussion about these transitions, which we call parasitic lines, will be presented in the Appendix.

As schematically displayed in Figure 1, potential energy surface (PES) with a more or less deep well and/or a repulsive PES may correlate with the NO ($^2\Sigma^+$, $v = 0$) + O ($^3P_2$) channel and thus with the observed narrow and broad unstructured transitions. The energy D_1 of this channel is reached via sequential 2-photon absorption if $h\nu_2 = D_1 - h\nu_1$. For example, on Figure 2 the arrow with the label D_1 indicates the ν_2 frequency that allows to reach D_1 when $h\nu_1 = D_0 - E_b = 25093.4$ cm^{-1}. This frequency ν_2, specific to each frequency ν_1, separates two very different kinds of transitions: (i) those occurring to bound states lying below D_1 (i.e., terminating on a binding final PES) which are expected to be sharp and (ii) those occurring to resonances or scattering states above D_1 (i.e., terminating on an attractive or repulsive final PES) which are expected to be broader (in the simplest case there is no barrier in the upper PES and D_1 is approached asymtotically).

We first examine those transitions originating from some loosely bound levels just below D_0 (relative energy $-E_b$) and terminating on bound levels lying below D_1 (relative energy $-E_b'$). Such bound−bound transitions are found on the low energy side in Figure 2 but are unfortunately somewhat covered by free NO lines. To identify and investigate them, we have rescaled the energy axis of the spectra to the final binding energy $E_b' = D_1 - h\nu_1 - h\nu_2$. This corresponds to a shift of each spectrum according to the change in binding energy E_b of the intermediate selected state (and in turn in ν_1). The 43 transformed spectra are presented in Figure 3, where the large intensity peaks belonging to cold NO have been truncated for clarity. In addition, the baseline of each spectrum has been shifted vertically in order to represent the binding energy E_b of the intermediate loosely bound states. In Figure 3 one clearly observes two families of lines: those which abscissa E_b' shifts linearly with E_b and those with fixed abscissa. Most of the numerous lines of the first type belong to the NO $\gamma(0,0)$ $\Omega = {}^1/_2$ transitions and appear at fixed ν_2 positions in Figure 2. As a matter of fact, following the formula given above for E_b', the NO lines move linearly in Figure 3 according to $E_b' = D_1 - (D_0 - E_b) - h\nu_2$, where ν_2 is the NO transition frequency. In the energy range displayed in Figure 3, the $\gamma(5,4)$ $\Omega = {}^1/_2$ transitions are not visible. Conversely, the very weak series of moving lines, starting at $E_b' = 50$ cm^{-1} for $E_b = 0$ cm^{-1} and vanishing around $E_b = 20$ cm^{-1}, correspond to NO $\gamma(5,4)$ $\Omega = {}^3/_2$ transitions (see Appendix). The much less numerous lines, appearing at fixed abscissa positions in Figure 3 for different values of E_b are assigned to bound−bound transitions. They can be traced as shown by the vertical arrows. An important characteristic of these transitions to the loosely bound levels below D_1 is that their density appears to be quite low, compared to what is observed 100 cm^{-1} below D_0, where $\rho \cong 0.5$ level/cm^{-1}. In addition, it is interesting to note that since the photon energies do not allow for production of electronically excited NO molecules, the fluorescence we observe in the experiment must be the fluorescence of highly excited (*quasi* bound) states of NO_2 lying just below D_1.

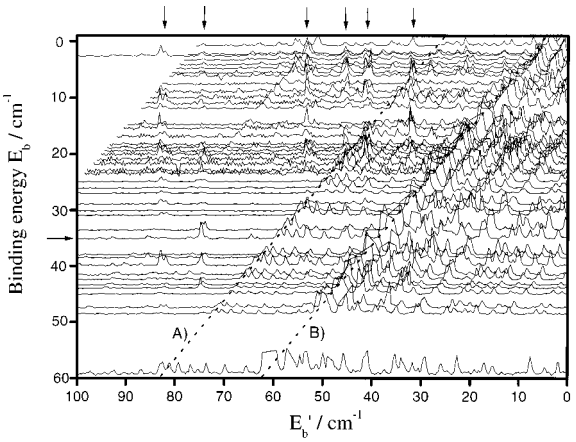

Figure 3. Ensemble of the 43 experimental spectra. The abscissa axis is the final bound energy $E_b' = D_1 - h\nu_1 - h\nu_2$. The ordinate axis gives the intermediate bound energy E_b of each 2-photon spectrum. The horizontal arrow on the left side marks the spectrum of Figure 2. The obvious bound−bound transitions (indicated by the vertical arrows) are those which occur to the same bound levels below D_1 for various intermediate loosely bound levels below D_0. Contrarily, the numerous lines moving linearly with E_b correspond to free NO transitions (they appear at fixed ν_2 positions on Figure 2 when ν_1 is varied). (A) and (B) mark lines that correspond to the $\gamma(0,0)$ $\Omega = {}^1/_2$ band. (A) in particular marks the band head (located at 44 175 cm^{-1} on Figure 2), while (B) corresponds to the three intense cold NO lines (truncated here) that appear at 44 200 cm^{-1} on Figure 2.

We now turn to the case of transitions occurring from the loosely bound states below D_0 to states lying above the dissociation channel NO ($^2\Sigma^+$, $v = 0$) + O ($^3P_2$). As displayed in Figure 2, the corresponding characteristic broad absorption typically expands over 100 cm^{-1} from D_1 to larger energies (still assuming that there is no barrier in this dissociation channel). We observed that in all cases the pump transition was saturated but the probe transition was not. Therefore, the observed intensities have been normalized *linearly* versus the recorded visible LIF signal (*proportional to the amount of NO_2 molecules excited below the threshold*) and versus the intensity of the probe laser. To focus on this spectral feature as a function of bound state energies and to separate it from the remaining narrow lines, we have represented these broad unstructured absorptions using a spline function, which is only an other representation of the primary data. Results of this procedure are displayed for several spectra in Figure 4. The underlying smooth dashed curves in Figure 4 are splines performed on typical sets of 10 points sampling the experimental envelope of the unstructured features. The systematic trend of this unstructured absorption feature for five different binding energies E_b can be recognized easily. In particular, we point out three characteristic phenomena of the broad absorption spectra depending on E_b: (i) the drift of the energy of the maximum, (ii) the change of the amplitude at the maximum, and (iii) the evolution of the overall shape of the feature. The drift of the energy of the maximum reflects mainly (but not only) the shift of the low energy edge of the unstructured feature, which corresponds to the minimum energy $h\nu_2$ for which the D_1 threshold is reached (depending on ν_1). Therefore, it is relevant to plot the broad UV-LIF absorption spectra versus the energy (E_{exc}) in excess above D_1 ($E_{exc} = h\nu_1 + h\nu_2 - D_1$) and versus

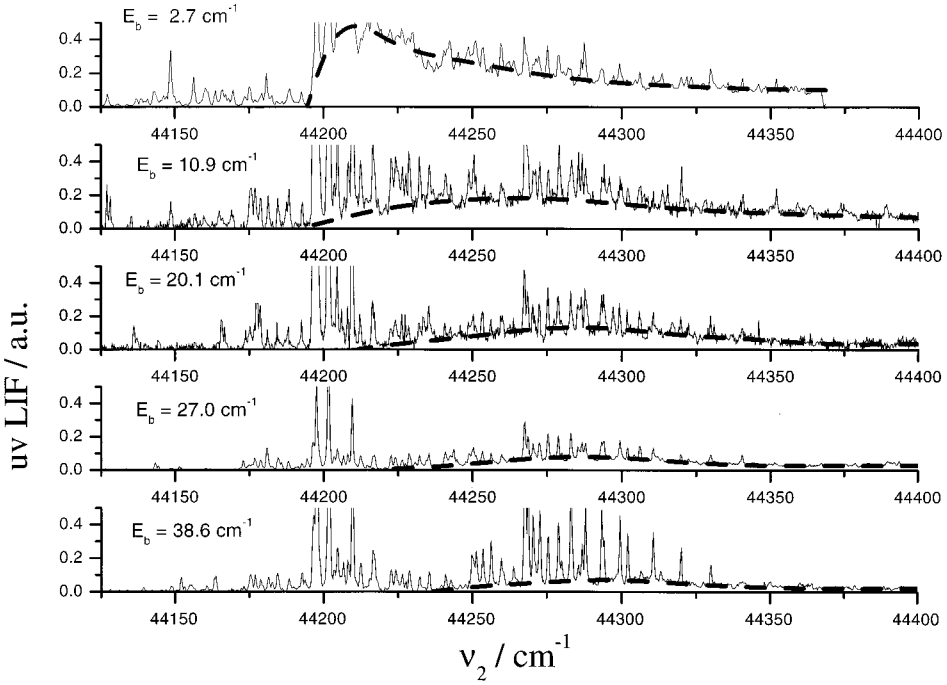

Figure 4. Example of 5 UV-LIF spectra recorded versus ν_2, for different bound energies $E_b = h\nu_1 - D_0$. E_b increases from top to bottom. The broad absorption feature is fitted with a spline.

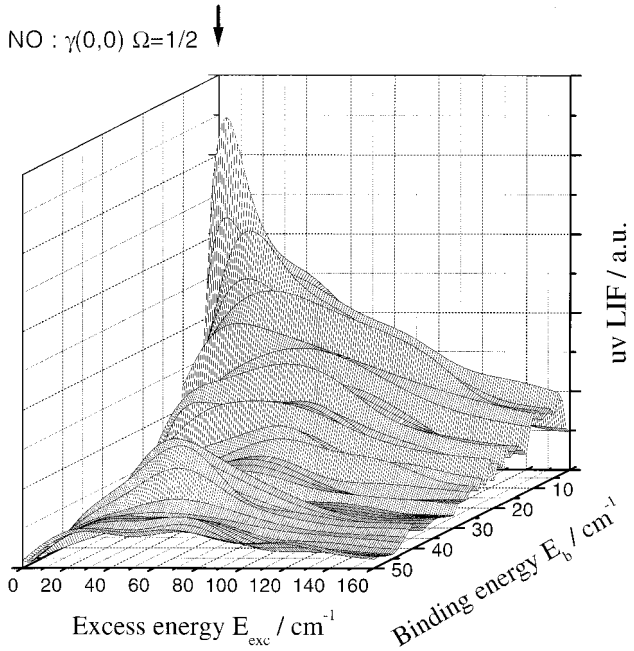

Figure 5. 3D representation of the fitted experimental broad absorption spectra, as a function of both the excess energy E_{exc} (above D_1) and the binding energy E_b (interpolated points sample regularly the E_b axis). One clearly observes the shift of the maxima, the broadening of the broad absorption feature and the drift in intensity. The vertical arrow locates the transition of free NO, $\gamma(0,0)$ $\Omega = {}^1/_2$.

the binding energy E_b, as shown in Figure 5 in a 3-D representation. While details of the change in the shape of the absorption feature is difficult to explain at the moment, it appears very clear that the effect and the signal is limited to the threshold region $E_0 > E > E_0 - 60$ cm^{-1}, a region where the molecule is most loosely bound. For larger binding energies this effect vanishes completely.

Let us summarize our observations. Vibrationally pre-exicted NO_2 is further electronically excited at a frequency ν_2 characteristic of the diatomic fragment NO. This transition is possible (i.e., the absorption is detected) only from the bound states of NO_2 lying in the immediate vicinity of the dissociation threshold. Our conclusion is that these *loosely bound* states exhibit properties inherent to the fragments of the NO_2 dissociation. What are the physical grounds for this strange behavior? Qualitative answer is based on the well-known fact that the potential along O···NO coordinate is barrierless. This means that as the internal energy of the bound molecule approaches D_0 ($E_b \rightarrow 0$), the average distance between oxygen and NO diatom may significantly increase. In fact, the outer turning point of the O···NO vibration tends to infinity when $E \rightarrow D_0$. As a result, vibrational wave functions spread over the dissociation coordinate and there is a nonvansihing probability of finding bound NO_2 in the asymptotic region of the potential, where fragments are nearly independent. The molecule becomes "floppy" and resembles a weakly bound complex. In such a case, Franck−Condon factors are favorable for selective excitation of the NO moiety at frequencies close to the free NO transition. As E_b increases, the outer turning point in the dissociation coordinate moves inward and the wave functions localize in the inner part of the potential. The NO moiety is no longer independent of the oxygen atom and NO_2 ceases to absorb light at the frequency of free NO. At this point it is interesting to make a remark about the fact that the broad component of the spectra does not saturate versus the probe energy (see above), while the $\gamma(0,0)$ transition of NO does easily saturate.[23] In fact, this can be seen as a consequence of the broadening of the absorption from the loosely bound states of NO_2, compared to free NO transition. In other words, the dilution of the oscillator strength of the NO chromophore wihin the highly excited states of NO_2 decreases the absorption cross section. A more in-depth analysis of the measured spectra is given in the next section.

B. Experimental Spectra and a Simple Dynamical Model. The aim of this section is to strengthen the conjecture that bound states with large expectation values of O···NO distance are detected near the dissociation threshold of the ground electronic state. Trustworthy modeling of the pump−probe experiment

requires accurate knowledge of at least three key parameters, namely the full dimensional potential energy surfaces of the initial and final electronic states and the transition dipole moment function. Using this input information, one can solve time-independent Schrödinger equation for the lowest electronic state, find the wave functions of highly excited vibrational states and, multiplying them with the dipole moment function, built initial wave packets on the final electronic state. Solving time-dependent Schrödinger equation for these initial wave packets, one simulates absorption spectra which can be compared with experiment. This scheme requires demanding "brute force" quantum calculations, but, once realized, it provides a deep insight into the molecular dynamics underlying the observed spectra. Numerous successful examples of such studies are discussed in ref 20.

Difficulty in interpretation of the NO_2 spectra measured in this work lies in the fact that very little is known about the PES's involved in the excitation. An exception is the lowest electronic state, X^2A_1, for which several PES's are available.[24−27] Ab initio calculations confirm the experimentally established fact that the O···NO potential has no barrier along the minimum energy path (MEP) connecting stable molecule and dissociation products O + NO. At the same time, none of the surfaces is accurate enough to correctly describe vibrational levels near the dissociation threshold. In particular, they fail to properly take into account the asymptotic interaction between products, which is expected to dominate the dynamics of loosely bound states. As for the excited electronic states lying 44 000 cm^{-1} above D_0 (which is roughly the frequency of the probe pulse), PES's for them have not been studied yet. In such a situation, we have to abandon the idea of accurate numerical simulation of absorption spectra and resort to semiempirical modeling. The goal is to trace the relation between the average distance O··· NO for a given vibrational level on the ground electronic state and the shape of the absorption spectrum measured for this level. Our approach is the following: First, the spectrum is analyzed, which is recorded for the bound level with $E_b = 2.7$ cm^{-1} (upper panel in Figure 4). Given a wave function for this level, we consider several trial potential functions for the final electronic state and select the one which yields the best fit to the measured spectrum. Next, when the upper state potential is fixed, all other spectra are included in the analysis. For every energy E_b we now vary the wave function on the ground electronic state until the agreement with the experimental spectrum is reached. With these wave functions, expectation values of the O···NO distance are calculated and studied as a function of E_b. As was already discussed in the preceding section, the observed transitions fall into two classes: narrow lines, attributed to bound levels on the upper electronic state (bound−bound transitions), and structureless absorption signifying excitation of the continuum states above the threshold energy D_1 (bound−free transitions). Ideally, narrow lines should provide information on eigenfrequencies and rotational constants for the highly excited electronic state. However, we are not able to assign these transitions or organize them into progressions. For this reason, we focus on simulating the broad absorption above D_1.

Let us start by choosing the potential for the upper state. Since structure and force constants of NO_2 in this state are unknown, we model the potential with a *one-dimensional curve* thus restricting the number of alternatives. The only considered coordinate is the O···NO distance R. Three trial potentials $V(R)$ are considered for the upper state (see Figure 6, upper panel).[28] They schematically represent three possible types of interaction between oxygen and the NO diatom: a potential with a deep well (Figure 6, left frame); a potential with a high barrier (Figure 6, middle frame); and a repulsive potential which supports no bound states (Figure 6, right frame). The harmonic frequency for the first two curves equals 1600 cm^{-1}. Each of the wells is about 3 eV deep; the barrier height is 1.2 eV. At large distances, the potentials smoothly go over into multipole interaction between oxygen and NO (see below). The asymptotic value of the potential energy is chosen to coincide with the threshold energy D_1.

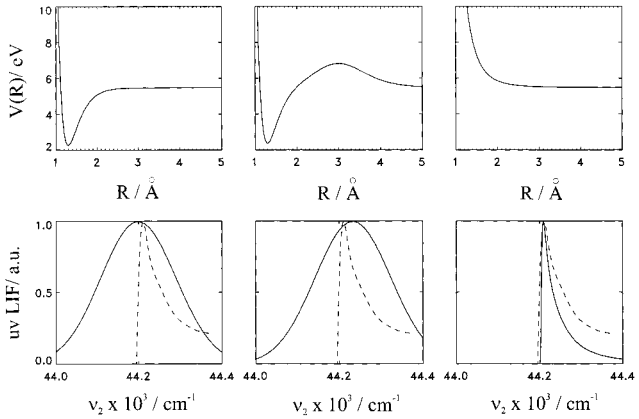

Figure 6. Upper panel: three trial potentials $V(R)$ for the upper state, used in fitting the experimental spectrum at 2.7 cm^{-1}. They schematically represent three possible types of interaction between oxygen and NO diatom: (i) a potential with a deep well; (ii) a potential with a high barrier; (iii) a repulsive curve which supports no bound states. Potential energy is measured with respect to the dissociation threshold D_0 of the ground electronic state. The asymptotic value of all three curves is taken to be 44 200 cm^{-1} Lower panel: absorption spectra (—), $\sigma(\nu_2)$, calculated as the Fourier transform of the time autocorrelation function, are compared with the experimental spectrum $\sigma_{exp}(\nu_2)$ (- - -, measured at $E_b = 2.7$ cm^{-1}) for comparison.

Wave functions of the loosely bound vibrational levels on the ground electronic state are the unknowns in the fitting procedure. Their shape was previously analyzed for a two-dimensional model which included the O···NO distance R and the bending angle γ.[8] It was shown that if the potential along R included long-range electrostatic interactions,

$$V(R \rightarrow \infty,\gamma) = A/R^4 + B/R^5 + C/R^6$$

the eigenfunctions developed pronounced maxima at large interfragment distances ($R \geq 7$ Å). In line with these results, we model the wave functions with a sum of two R-dependent Gaussians, whose positions, widths, and amplitudes have to be found in the nonlinear fit. One Gaussian describes the molecule in the inner part of the potential and the other one measures the probability density at large O···NO separations. The reason for this rather crude approximation has an experimental origin: since the bandwidth of the pump laser ($\approx$0.3 cm^{-1}) is larger than the average level spacing in the vicinity of D_0 (the density of states is $\approx$10 levels/cm^{-1}), we excite not a single eigenstate, but a group of loosely bound levels. The trial wave functions represent these initial wave packets.

The initial wave packet is placed on one of the upper potential curves and propagated using one-dimensional time evolution operator. The transition dipole moment is assumed to be constant. The absorption spectrum, $\sigma(\nu_2)$, calculated as a Fourier transform of the time autocorrelation function,[20] is then compared with the spectrum $\sum_{exp}(\nu_2)$ (measured at $E_b = 2.7$ cm^{-1}) at a set of 20 representative points.[29] Using nonlinear least-squares fit we search for the parameters of the initial wave packet which minimize the difference $|\sigma(\nu_2) - \sigma_{exp}(\nu_2)|$. The

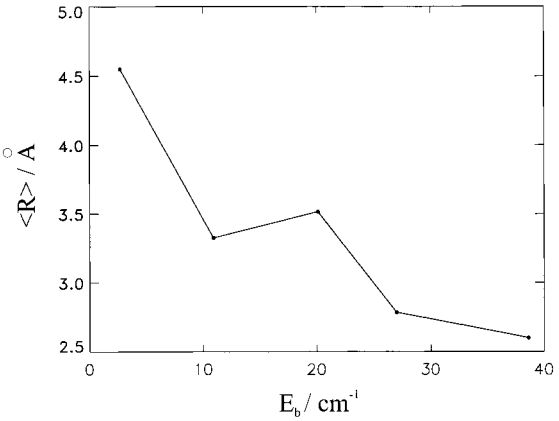

Figure 7. Expectation values $\langle R \rangle$ for the initial wave packets, providing the best fit, as functions of the energy E_b of loosely bound states.

results of this assessment for three trial potentials are shown in Figure 6 (lower panel). It is clear that the repulsive curve provides the best fit. The initial wave packet in this case is located in the asymptotic region, the average O···NO distance being $\langle R \rangle \approx 5$ Å. Particularly striking is the agreement at small energies near the threshold D_1, where $\sigma_{exp}(\nu_2)$ sharply rise from zero to the maximum value. Simulated absorption is asymmetric with respect to D_1 because the repulsive potential has no bound states. In contrast, absorption spectra for the potentials with minimum behave smoothly at D_1 and are nearly symmetric, because the initial wave packet is projected on both bound and continuum states of the upper surface.

The repulsive curve is further employed in fitting of the other four spectra shown in Figure 4. Here, too, the experimental absorption can be reproduced reasonably well. Expectation values $\langle R \rangle$ for the initial wave packets, providing the best fit, are plotted in Figure 7 against the energy E_b of loosely bound states. At the threshold, the most probable distance O···NO is very large. As E_b increases, $\langle R \rangle$ shortens. The reason is that the maximum of absorption in the experiment gradually shifts to higher energies with growing E_b (cf. Figure 4). As a result, trial wave functions are pushed to smaller R values where the repulsive potential is also higher.

Thus, the observed spectra are sensitive to the shape of wave functions of loosely bound states along the dissociation coordinate. Within the considered model, intense background absorption points to the existence of unusual threshold states with large O···NO separations. Of course, this is merely an *indication*, not a proof, that these states are indeed detected in our experiment: the model is far too simplistic. Let us briefly review the most important effects which were intentionally disregarded in the above discussion. First, modes in NO_2 are strongly coupled and a one-dimensional approximation is not satisfactory. Additionally, transition dipole moment is obviously coordinate dependent and this should be taken into account. One can argue that it is this coordinate dependence that leads to decrease of absorption with growing E_b, as observed on Figures 4 and 5 (in fact, it is the integrated absorption that must be compared with the transition dipole moment). Second, it remains unknown if the bound−bound and bound−free transitions terminate on the same upper electronic state. The above model suggests that a least two different electronic states must be involved, one for narrow bound lines and the other one for the structureless absorption. This is, however, unprovable. The model favors a repulsive potential because only broad background, corresponding to a direct decay, is included in the analysis. It is also not clear if some resonance states are excited above D_1. Their detection could help to make the choice of the potential for the upper state less arbitrary. Finally, we have virtually no information about the genesis of delocalized wave functions of probed states. They can result from the asymptotic part of O···NO interaction, as suggested above. However, there exist many excited electronic states which at large R are nearly degenerate with the ground-state $\tilde{X}^2A_1$. These may have shallow minima accessible in optical transitions from the ground state.[25,30,31] Therefore, we cannot rule out the possibility that we probe these long range parts of the electronically excited states.

C. Spectral Features of Loosely Bound States in a Chemically Bound Molecule and a van der Waals Complex. In this section we would like to point out and discuss the apparent analogy of spectra (A ← X transition) of the NO−Ar van der Waals complex[32,33] and loosely bound NO_2 molecules. In the case of the NO/Ar complex two electronic states (which are weakly bound) contribute to the electronic A−X spectrum. This electronic system has been reinvestigated recently, showing that two kinds of transitions, occurring from a bound vibrational level of the electronic ground state (correlated with the $\tilde{X}^2\Pi$ state of NO) to the first electronic excited state (correlated to the $\tilde{A}^2\Sigma$ state of NO) can be observed.[33] Transitions terminating on the repulsive part of the upper PES (bound−free transitions) and transitions terminating on a bound vibrational levels of the upper PES can be easily distinguished because of their different spectral features. As opposed to the narrow bound−bound transitions, the bound−free transitions for NO−Ar complexes correspond to a broad unstructured feature shifted to the blue. As we have discussed above the same kinds of transitions have been observed between the loosely bound levels of NO_2 lying below D_0 and the electronic excited states correlated with the $A^2\Sigma$ state of NO. In other words, a loosely bound NO_2 molecule appears to possess properties which are close to a van der Waals complex (NO−Ar for instance).

An interesting question related to the dynamics of loosely bound states is: how do these "exotic" states behave in collisions? In recent experiments Bieler et al.[34] have investigated the collisional activation of loosely bound molecules just below D_0 in a crossed molecular beam to measure energy transfer properties (like the average energy transferred in a collision $\langle \Delta E \rangle$). Activating collisions cause loosely bound NO_2 molecules to decompose and the event and extent of energy transfer can be monitored through the state resolved detection of the dissociation product. Surprisingly, it has been found that the product state distributions of NO after NO_2/Ar and NO/Ar collisions were surprisingly similar.[34] This also supports the picture that the loosely bound NO_2 molecules close to D_0 resemble a "two fragment complex", with one nearly unexcited NO spectator bond.

D. Density of States Close to D_0. It has been well documented that the density of states close to the dissociation threshold D_0, derived from the density of lines in this particular region, is much higher than expected.[6,7] In comparison to extrapolations from lower energies there appears to be a mismatch of a factor of 4−5. The reason for this behavior is not completely clear at present. One explanation for this phenomenon may be the long-range tail of the ground-state potential. However, the "density of states problem" was the motivation for suggesting that very close to (but below) D_0 there may exist (in addition to "normal" mixed states) a family of vibrational levels (of the ground-state PES) corresponding to large amplitude motions of almost free rotation of an O atom around the NO occurring at large average "interfragment"

distances (|O...NO| > 7 Å) which could account for the observed phenomenon. Another explanation for the observed density of states, however, could be the various excited states potential energy surfaces, being almost degenerate at large *R*, which correlate with NO ($^2\Pi_{1/2}$) and O ($^3P_2$) and which may have shallow minima and thus contribute significantly to the experimental density of states. As stated above, with our experimental data at present we cannot judge whether measured spectra, the features of the loosely bound states and the strikingly high density of states are governed by the long-range part of the ground-state PES or the features of the various excited-state PESs. However, even if we cannot prove or disprove these possibilities, we believe that the phenomenon we observe must have something to do with the appearance of the unusual density of states. Both effects are largest close to D_0 and vanish at energies of about 60 cm^{-1} below D_0. In addition, we want to emphasize that an explanation for the density of states problem based upon the long range part of the ground state potential is the simplest (theoretically feasible) approach which appears to work already reasonably well (at least *semi*quantitatively).[8] However, this still does not rule out significant contributions of excited states. In any case theoretical approaches taking these states into account are much more difficult.

Summary and Conclusions

In this paper we have shown that the bound states located in the vicinity of the first dissociation threshold of NO_2 ($E_b/D_0 \cong 10^{-3}$) absorb photons in an energy range close to the one at which free NO molecules absorb. In our particular experiment we probed the NO electronic "chromophore" within the bound states of NO_2 lying in the vicinity of its first dissociation threshold, located at $D_0 = 25\,128.57$ cm^{-1}. The main result of the experiments reported here is that, the smaller the binding energy, the closer to free NO transitions is the excitation spectrum from the loosely bound states of NO_2 to some unknown excited state(s). Most of the absorption from the loosely bound states occur to a dissociative state, so that most of the corresponding spectrum is broad and unstructured, with an increasing shift to the blue as the binding energy increases. Very weak bound − bound transitions are also observed. In this paper we are describing an experimental strategy to probe loosely bound states in highly excited NO_2 very close to the first dissociation threshold D_0. We have shown that many of the very loosely bound states of the NO_2 can be understood in terms of a simple local mode picture where the states correlate with a motion of two fragments, NO and O, "orbiting" around each other. Consequently, most of the energy (or the energy of most of the states) is shared between the dissociation coordinate and the hindered rotor, with no excitation of the NO spectator bond, allowing for large amplitude motions between NO and O. This implies that the loosely bound states exhibit spectroscopic features close to those of the fragments (i.e., absorption in the asymptotic limit of the PES). This property, that we think may be quite general for triatomics, can be related to the long-range interactions between NO and O. *On the other hand we expect that this effect will be restricted to low J quantum numbers of the parent molecule because for higher J rotational barriers will exclude the long-range part of the PES.* We have pointed out the strong analogy between such a description and the features of weakly bound van der Waals complexes, like NO−Ar for instance. More generally, we suggest in this article that many chemically bound molecules (ABC) may behavelike a weakly bound complex AB...C when excited very close to their dissociation threshold. Just recently Schinke et al.[35] have theoretically investigated loosely bound states of HOCl (very close to the dissociation threshold) which to some extent resemble the weakly bound states in NO_2 discussed here. However, even if this concept is rather the rule than the exception, one may anticipate that often strong selection rules and weak FCFs prevent to observe such states. In principle, Stimulated Emission Pumping experiments should be particularly well suited for probing loosely bound vibrational states of polyatomics but we are not aware of any experiment in the literature in this direction. From an experimental point of view, the case of NO_2 may be rather exceptional because simple direct excitation of all the loosely bound states can be performed, due to very strong vibronic and rovibronic intramolecular couplings between the levels of the electronic ground state and the first electronically excited state, making nearly all the highly excited dark states of the ground state as observable as those of the "bright" $\tilde{A}^2B_2$ state.

Acknowledgment. Stimulating discussions with R. W. Field, R. Jost, and J. Troe as well as financial support from the Deutsche Forschungsgemeinschaft within the SFB 357 ("Molekulare Mechanismen Unimolekularer Prozesse") are gratefully acknowledged. F.R. and S.Y.G. thank the "Fonds der Chemischen Industrie" and the *Alexander von Humboldt-Stiftung* for a fellowship. Finally, A.D. is grateful for partial support from a NATO fellowship. The partial support from the PROCOPE program is acknowledged. The Grenoble High Magnetic Field Laboratory is "Laboratoire conventionné aux universités UJF et INP de Grenoble".

Appendix

In this Appendix we give more information about the parasitic NO lines which are superimposed on the $\nu_1 + \nu_2$ spectra discussed in section III. Basically, two facts are responsible for these parasitic lines: (i) the presence of free NO in the supersonic jet and (ii) the sequential 2-photon excitation and dissociation ($2\nu_1$ transitions) of NO_2.

It is well-known that a major problem in NO_2 photodissociation experiments is background NO due to wall-catalyzed NO_2 decomposition. This contribution has been verified by recording the UV-LIF spectra when only the probe laser was on. Because NO is also cooled in the jet down to about 2 K, in this case mainly the partially saturated $R_{11}(^1/_2)$, $Q_{11}(^1/_2)$, and $^SR_{21}(^1/_2)$ transitions of the $\gamma(0,0)$ band of NO were observed. These three intense lines, located around 44 200 cm^{-1} appear in every spectrum and can be hardly avoided. They can be used as internal frequency standards and as references for calibration.

Unfortunately, the experimental spectra obtained in this study show numerous sharp lines on both the blue and red side of the three "cold NO" lines at 44 200 cm^{-1}, which have nothing to do with spectral properties of loosely bound states. Fortunately, as pointed out in section III, an easy way to distinguish the latter transitions from the parasitic lines is the investigation of their dependence on the pump laser frequency ν_1.

Almost all the lines spreading from 44 175 to 44 250 cm^{-1} have been assigned to NO $\gamma(0,0)$ lines originating from $\Omega = {}^1/_2$ with J up to typically $^{17}/_2$.[13] Their intensities vary approximately linearly with the pump energy and are partially saturated against the probe energy. The origin of these lines is a hardly avoidable sequential 2-photon photodissociation of NO_2: (i) the first ν_1 step (strongly saturated) promotes the molecules to some loosely bound states; (ii) the second ν_1 step excites the molecule to some very short lifetime resonances around 50 000 cm^{-1}, therefore inducing fast photodissociation;

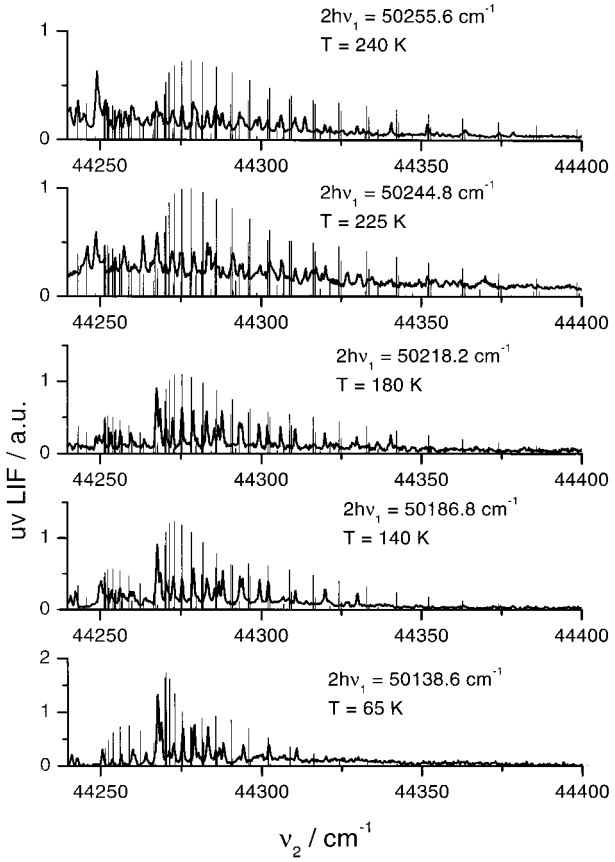

Figure 8. Fractions of spectra between 44250 and 44400 cm^{-1}. The $\gamma(5,4)$ rotational lines of NO (picked fence) are simulated (not fitted) by using a rotational temperature given by $kT = 2h\nu_1 - 50096.4\ cm^{-1}$.

(iii) the last ν_2 step probes the product NO ($^2\Pi_{1/2}$, $v = 0$) and is partly saturated. Note that the 3 intense lines at 44200 cm^{-1} have two contributions: ν_2 processes (without pump) detecting wall-catalyzed NO_2 decomposition and sequential 2-photon photodissociation of NO_2 and NO detection ($2\nu_1 + \nu_2$).

The lines spreading from 44 250 cm^{-1} and expanding further to the blue side are partly saturated NO $\gamma(5,4)$ transitions originating from $\Omega = {}^1/_2$. The general trend of the $\gamma(5,4)$ rotational envelope can be easily understood. This is due to the fact that the energy of the dissociation channel NO ($^2\Pi_{1/2}$, $v = 5$, $J = {}^1/_2$) + O ($^1D_2$) is located 24 967.7 cm^{-1} above the first dissociation threshold D_0 (the vibrational energy of the level $X^2\Pi_{1/2}$, $v = 5$, $J = {}^1/_2$ is 9099.91 cm^{-1}).[36] This corresponds to a total energy of 50 096.4 cm^{-1}, which is accidently close to $2h\nu_1$: see Figure 1. To confirm this interpretation, we have checked that the $\gamma(5,4)$ transitions disappear when ν_1 becomes smaller than ${}^1/_2(50\ 096.4) = 25\ 048.2\ cm^{-1}$, the minimum energy for which the channel NO ($^2\Pi_{1/2}$, $v = 5$, $J = {}^1/_2$) + O ($^1D_2$) is open. Conversely, when $h\nu_1 = D_0$ the excess energy available for rotation and translation is 161 cm^{-1}. One can observe in Figure 8, were five spectra in the region of the prominent $\gamma(5,4)$ lines of the NO spectrum, that the rotational envelopes are roughly reproduced by a simulation of the NO spectrum assuming a rotational temperature given by $kT = 2h\nu_1 - 50\ 096.4\ cm^{-1}$.[36] The "temperature" (depending on the excess energy of NO) ranges from 240 to 65 K when the pump energy varies from 25 127.8 to 25 069.3 cm^{-1}. Note that we did not make any attempt to spectroscopically fit the lines but to show the reasonable semiquantitative agreement. Therefore, a precise match of the positions of the observed and calculated lines cannot be perfect. Finally, it is interesting to remark that a similar additional channel, NO ($^2\Pi_{3/2}$, $v = 5$, $J = {}^3/_2$) + O ($^1D_2$), corresponding to the upper spin-split level of NO, is located 25 086.7 cm^{-1} above D_0. Therefore, as soon as ν_1 is larger than ${}^1/_2(25\ 086.7 + D_0) = 25\ 107.6\ cm^{-1}$ (that is for E_b smaller than 21 cm^{-1}), such lines could appear, shifted by about 120 cm^{-1} to the red side relative to those spreading from 44 250 cm^{-1}. Their corresponding rotational temperature is of course lower (at most 42 K when $h\nu_1 = D_0$). These lines can conveniently be observed in Figure 3, where they correspond to the moving features (on the left side of the NO $\gamma(0,0)$ band head) that disappear for binding energies E_b larger than about 20 cm^{-1}.

References and Notes

(1) Nesbitt, D. J.; Field, R. W. *J. Phys. Chem.* **1996**, *100*, 12735.
(2) Baer, T.; Hase, W. L. *Unimolecular Reaction Dynamics*; Oxford University Press: Oxford, New York, 1996.
(3) Abel, B.; Hamann, H. H.; Lange, N. *Faraday Discuss.* **1995**, *102*, 147.
(4) Delon, A.; Georges, R.; Jost, R. *J. Chem. Phys.* **1995**, *103*, 7740.
(5) Georges, R.; Delon, A.; Jost, R. *J. Chem. Phys.* **1995**, *103*, 1737.
(6) Jost, R.; Nygard, J.; Pasinski, A.; Delon, A. *J. Chem. Phys.* **1996**, *105*, 1287.
(7) Delon, A.; Heilliette, S.; Jost, R. *Chem. Phys.* **1998**, *238*, 465.
(8) Grebenshchikov, S. Y.; Delon, A.; Heilliette, S.; Schinke, R.; Jost, R. to be published in *Z. Phys. Chem.*
(9) Stone, A. J. *The theory of intermolecular forces*; Oxford University Press: Oxford, U.K., 1996.
(10) LeRoy, R. D.; Charley, J. S. *Adv. Chem. Phys.* **1980**, *42*, 353.
(11) Fleming, P. R.; Li, M.; Rizzo, T. R. *J. Chem. Phys.* **1991**, *95*, 865.
(12) Fleming, P. R.; Li, M.; Rizzo, T. R. *J. Chem. Phys.* **1991**, *94*, 2425.
(13) Reisel, J. R.; Carter, C. D.; Laurendeau, N. M. *J. Quant. Spectrosc. Radiat. Transfer* **1992**, *47*, 43.
(14) Le Roy, R. J.; Bernstein, R. B. *J. Chem. Phys.* **1970**, *52*, 3869.
(15) Le Roy, R. J. *J. Mol. Spectrosc.* **1973**, *1*, 113.
(16) Field, R. W. *Colloq. Int. CNRS* **1970**, *273*, 143.
(17) Lievin, J.; Delon, A.; Jost, R. *J. Chem. Phys.* **1998**, *108*, 8931.
(18) Note that in the case of a symmetric triatomic molecule, such as NO_2, the two oxygen atomes have equal probabilities to explore large R and γ, as opposed to an asymmetric molecule.
(19) Bashkin, S.; Stoner, J. O., Jr. *Atomic Energy Levels and Gotrian Diagrams Vol1*; North-Holland Publishing Company: Amsterdam, 1975.
(20) Schinke, R. *Photodissociation Dynamics*; Cambridge University Press: Cambridge, U.K., 1993.
(21) Abel, B.; Lange, N.; Reiche, F.; Troe, J. *J. Chem. Phys.* **1999**, *110*, 1389.
(22) Abel, B.; Lange, N.; Reiche, F.; Troe, J. *J. Chem. Phs.* **1999**, *110*, 1404.
(23) Cunge, G.; Booth, J. P.; Derouard, J. *Chem. Phys. Lett.* **1996**, *263*, 645.
(24) Klippenstein, S. J.; Radivoyevitch, T. *J. Chem. Phys.* **1993**, *99*, 3644.
(25) Katagiri, H.; Kato, S. *J. Chem. Phys.* **1993**, *99*, 8805.
(26) Harding, L. B.; Stark, H.; Troe, J.; Ushakov, V. G. *Phys. Chem. Chem. Phys.* **1999**, *1*, 63.
(27) Grebenshchikov, S. Y.; Beck, C.; Flöthmann, H.; Schinke, R.; Kato, S. *J. Chem. Phys.* **1999**, *111*, 619.
(28) We do not cite analytic expressions for the potential functions: On one hand, they are looking cumbersome, and on the other hand our analysis is almost qualitative and does not rely on the exact shape of $V(R)$—any set of functions which reproduce the general run of the curves in Figure 7 will give similar results.
(29) Since the dipole moment function is assumed to be constant, we cannot fit the amplitude of the absorption spectrum. For this reason both experimental and calculated spectra are renormalized before comparison in such a way that their amplitude at maximum of absorption equals unity.
(30) Mikhaylichenko, K.; Wittig, C. *Chem. Phys. Lett.* **1998**, *287*, 209.
(31) Ionov, P. I.; Bezel, I.; Ionov, S. I.; Wittig, C. *Chem. Phys. Lett.* **1997**, *272*, 257.
(32) Langridge-Smith, P. R. R.; Carrasquillo, M.; E.; Levy, D. H. *J. Chem. Phys.* **1981**, *74*, 6513.
(33) Shafisadeh, N.; Brechignac, P.; Dyngaard, M.; Fillion, J. H.; Gauyacq, D.; Miller, J. C.; Pino, T.; Raoult, M. *J. Chem. Phys.* **1998**, *108*, 9313.
(34) Bieler, C.; Reisler, H. *J. Chem. Phys.* **1996**, *100*, 3882.
(35) Weiss, J.; Hauschildt, J.; Grebenshchikov, S. Y.; Dueven, R.; Schinke, R.; Koput, J.; Stamatiadis, S.; Farantos, S. C. *J. Chem. Phys.* **2000**, *112*, 77.
(36) Gundlach, G. Rechnen und Darstellen von Laserinduzierten Fluoreszenz Anregungsspektren des NO; DLR-Institut für experimentelle Strömungsmechanik, Göttingen, 1991.